Full Paper

Propellants, Explosives, Pyrotechnics

DOI: 10.1002/prep.201800126

A New Equation of State for Detonation Products of RDX-Based Aluminized Explosives

Yan Liu,*[a] Hong-fu Wang,[a] Fan Bai,*[a] Feng-lei Huang,[a] and Tariq Hussain[a]

Abstract: In order to explain the detonation performance of RDX-based aluminized explosives with different aluminum particle sizes, a new equation of state (EOS) for aluminized explosives is proposed. The proposed EOS regards the gasification of aluminum particles as a real reaction. The proposed EOS takes account of constituent aluminum particle sizes. The proposed EOS was implemented in LS-DYNA as a user defined EOS and validated by simulating the experiments of metal plates acceleration caused by detonation of RDX-based aluminized explosives. The numerical results reproduce the experimental finding that the reaction rate of aluminum particles increases with the decrease of aluminum particle size. The proposed EOS has several advantages over the previously reported equations of state for aluminized explosives. The reaction rate of aluminum constituents is calculated theoretically from their gasification reaction rate equation eliminating the need for experimental calibration of the corresponding empirical parameters.

Keywords: Aluminized Explosives · Aluminum Particle size · Equation of State · Reaction rate · Numerical Simulation

1 Introduction

Owing to their characteristics such as high detonation heat and temperature etc., aluminized explosives are widely used in various applications. The aluminized explosives have longer detonation reaction zones on base of which these are classified as typical non-ideal explosives [1–2]. In fact the addition of aluminum particles can improve the work capacity of the explosives, which is quantified by the equation of state (EOS) of the detonation products. The Jones-Wilkins-Lee (JWL) state equation is a classic empirical EOS [3], which is mostly used in evaluating the acceleration of metal plate driven by the detonation products. The standard form of JWL equation of state based on Jones and Wilkins' work is as follows:

$$p = A\left(1-\frac{\omega}{R_1 v}\right)\mathrm{e}^{-R_1 v} + B\left(1-\frac{\omega}{R_2 v}\right)\mathrm{e}^{-R_2 v} + \frac{\omega E}{v}, \quad (1)$$

where p is the detonation product pressure; v is the relative specific volume; E is the internal energy of the product; A, B, R_1, R_2 and ω are the coefficients obtained by empirical fitting on the cylinder test data [4]. However, due to subsequent reactions and even multiple reactions involving aluminum particles, aluminized explosives have particular structure of chemical reaction zone such as greater width and non-uniform temperature distribution. In an experiment, Finger et al. [5] observed that the aluminum particles of RDX-based aluminized explosives began to react after the detonation about in 5μs ~ 100μs. It was observed that during this time period, the energy released by the secondary reaction of aluminum particles did not directly contribute to accelerate the tube wall in the cylinder test. This implied that the state of the detonation products cannot be fully described by the JWL EOS.

Various studies on JWL EOS for aluminized explosives have been reported. Chen et al. [6] conducted an Ø50 mm cylinder test on aluminized explosives and calibrated the parameters of EOS of the aluminized explosives. Ji et al. [7] determined the JWL EOS of the aluminized explosives by Ø25 mm and Ø50 mm cylinder tests, and obtained the relation between the charge size and the work ability. Guo et al. [8] tested the metal accelerating ability of TATB based aluminized explosives and concluded that the compositions with smaller sized aluminum particles could impart greater velocities and acceleration in copper flyer plates. Baker et al. [9] added a term into JWL EOS to account for the aluminum reactions in the aluminized explosives in order to describe the expansion of detonation products. Philip J Miller [10] proposed a detonation reaction model of aluminized explosives to account for the combustion rate of aluminum particles after CJ point. The Miller extension in a JWL EOS for aluminized explosives is given by [16]

$$p = A\left(1-\frac{\omega}{R_1 v}\right)e^{-R_1 v} + B\left(1-\frac{\omega}{R_2 v}\right)e^{-R_2 v} + \frac{\omega(E+\lambda Q)}{v}, \quad (2)$$

[a] Y. Liu, H.-f. Wang, F. Bai, F.-l. Huang, T. Hussain
State Key Laboratory of Explosion Science and Technology, Beijing Institute of Technology, Beijing 100081, P.R. China
*e-mail: liuyan@bit.edu.cn
lg4700@163.com

where Q is the heat released by the reaction of aluminum particles, λ is the degree of reaction of aluminum particles. The slow reaction rate equation for the combustion of aluminum particles in detonation products is given by

$$\frac{d\lambda}{dt} = a(1-\lambda)^m \cdot p^n, \tag{3}$$

where the constant a is the dependence on the particle size; m and n are the reaction rate exponents. These parameters depend upon the characteristics of the explosives, such as the particle shape and size of the constituent aluminum particles, and calibrated by empirical fit on experimental data.

Yang et al. [11] calculated the blast of the aluminized explosives in concrete by using the JWL-Miller EOS. However, the calculated metal rod velocity was not in good agreement with the experimental value. Zhou et al. [12] also adopted JWL-Miller EOS to calculate the shock wave pressure of aluminized explosives in air. However, the velocity curve of the metal rod driven by detonation of aluminum explosives clearly deviated from the experimental value. The calculation and experimental results show that the calculated velocity is higher during first 1μs and lower afterwards than that in the experiment. The reason should be that the equation of state does not always completely reflect the actual situation of the aluminum particles reaction in the detonation of the aluminized explosives. Ripley et al. [13] added the crushing model of aluminum powder to the detonation process and calculated the shock wave pressure of the explosion of aluminized explosives in air. The calculated results are basically in agreement with the experimental results. The research of Pei [14] shows that aluminum particles were gasified before complex chemical reactions occurred. The reaction time of aluminum particles ranged from a few microseconds to a few tens of microseconds. It was therefore inferred that an EOS of detonation products that could describe the secondary reactions of aluminum particles would be of great significance to study the work capacity of aluminized explosives.

This paper proposes a new equation of state for detonation products of aluminized explosives which combines the vaporization rate of aluminum particles in detonation products with the traditional JWL equation. The new EOS is implemented in LS-DYNA as a user-defined EOS to simulate the aluminized explosives driven flyer experiments [15] with different aluminum particle sizes. Based on the new EOS, the reaction mechanism of aluminum particles in detonation products of aluminized explosives is investigated and the reaction rate for aluminum with different particle sizes is studied.

2 Experiment on Flyer Plate Driven by Aluminized Explosives

The experiment of explosives driving a metal plate is an effective method to investigate the explosives capacity and reaction progress of aluminized explosives. In the small charge experiments, the VISAR are used to observe the details of the metal plates driven by aluminized explosives with different formulations. This provides a simple and economical method for studying the detonation of aluminized explosives. Fortunately, in literature [15], the experiments of metal plates driven by a set of RDX aluminized explosive formulations with particle size ranged from tens of nanometers to a few hundred microns are studied. The diameter of the cylindrical aluminized explosive is 40 mm, and the length is 15 mm, and the thickness of the copper flyer is 1 mm. The experimental setup is shown in Figure 1; further details could be found in Ref [15]. Table 1 lists four formulations of the RDX-based aluminized explosives. Formulation 4 uses the LiF instead of aluminum particles because the mechanical properties of LiF are similar to that of aluminum, and LiF remains inert in the detonation process. Therefore, formulation 4 can describe the detonation performance of the aluminized explosives without aluminum particles participating in reactions.

Figure 2 (a) shows the velocity-time curves obtained by experiments of the copper plates resulting from the deto-

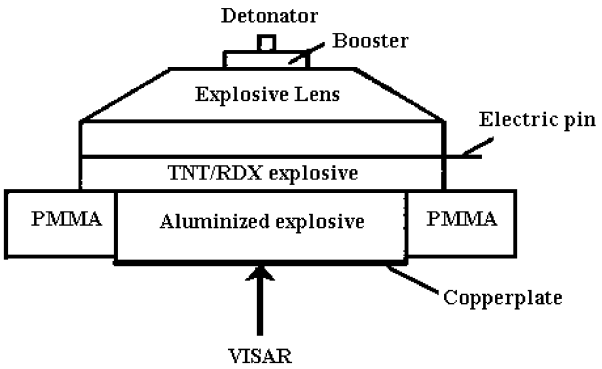

Figure 1. Experimental setup.

Table 1. Compositions of aluminized explosives.

Formulation No.	Composition	Aluminum particle diameter/μm
1	RDX(76%) + Al(20%) + Binder(4%)	0.05
2	RDX(76%) + Al(20%) + Binder(4%)	5
3	RDX(76%) + Al(20%) + Binder(4%)	50
4	RDX(76%) + LiF(20%) + Binder(4%)	Nil

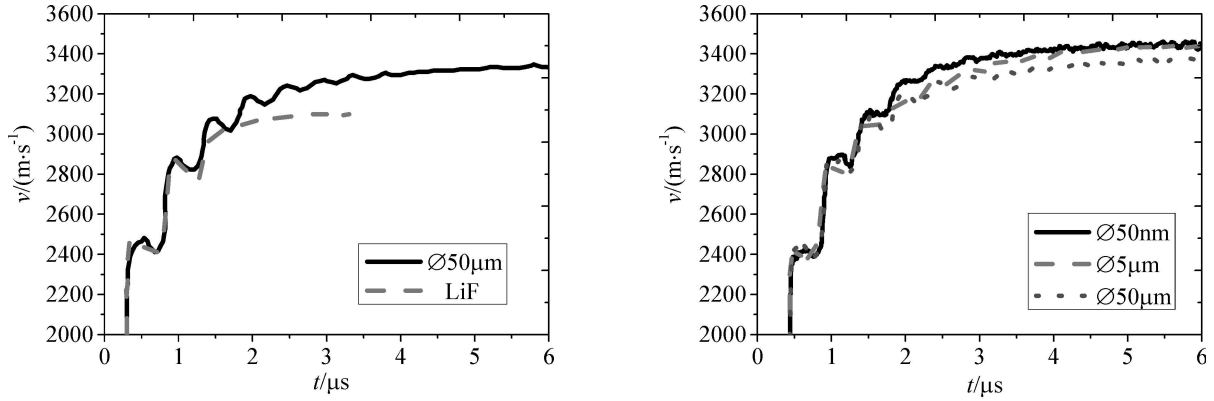

(a) *v-t* curves of on copper plate free surface (b) Free surface particle velocity of copper plate

Figure 2. Free surface velocity of 1 mm-thick copper plate.

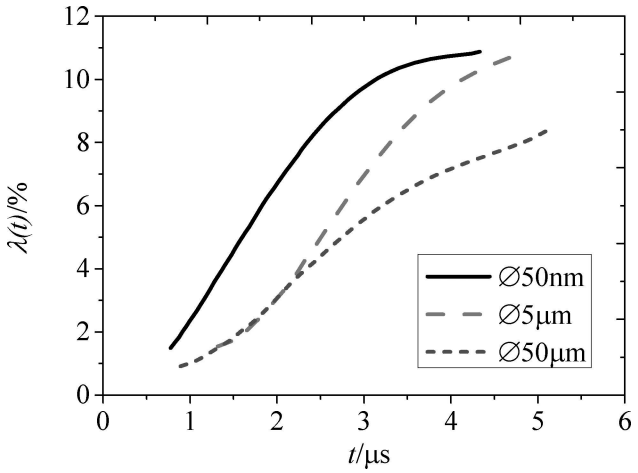

Figure 3. Reaction degree of aluminum particles in different aluminum particle sizes.

nation of formulation 3 ($\varphi = 50$ μm) and formulation 4 (LiF). Figure 2 (b) shows the free surface velocity of the 1 mm thick copper plates of driven by the formulation 1 ($\varphi =$ 0.05 μm), formulation 2 ($\varphi = 5$ μm) and formulation 3 ($\varphi =$ 50 μm).

In the experiments, the LiF keep inert during the explosive detonation in formulation 4, the kinetic energy of the copper is completely the contribution of detonation energy from the RDX explosive. In other formulations, except the energy of RDX, there is also the energy released by aluminum particles to the copper plate flying. By subtracting the kinetic energy of the copper plate driven by the aluminized explosive formulations (1, 2 and 3) from that of LiF explosive (formulation 4), the useful work from the energy released by aluminum particles reaction is obtained. The reaction rate curves of aluminum particles can thus be plotted. The degrees of reactivity $\lambda(t)$ of the aluminum particles with different particle sizes given in literature [15] are shown in Figure 3.

3 Determination of Equation of State Parameters

3.1 Determination of JWL State Equation Parameters for Ideal Component

The JWL EOS parameters of the RDX-based aluminized explosive formulations under consideration in this paper are the same as the formulation 4, in which the aluminum particles are replaced by LiF. In the literature [17], the parameters of JWL EOS for RDX explosives containing LiF are calculated by using the VLWR (modified VLW EOS), and are reproduced in Table 2.

The RDX explosives with LiF (formulation 4) driving flyer experiments were simulated by using LS-DYNA by modeling a two-dimensional axisymmetric structure. The diameter of the cylindrical explosive was 40 mm, and the length was 15 mm, the diameter of the copper flyer was 40 mm and the thickness was 1 mm. The grid size was taken as 0.2 mm per cell. The simulation setup is shown in Figure 4.

Table 2. Parameters of JWL equation of state for RDX composition in aluminized explosive.

Explosive	Method	ρ/(g·cm^{-3})	v/(m·s^{-1})	A/GPa	B/GPa	R_1	R_2	ω
LiF	VLWR	1.823	7903	459.687	21.751	4.5658	1.8367	0.5
	Simulation	1.823	7903	852	21	4.31	1.3	0.33

In the numerical simulation, the parameters of VLWR [6] are applied to the explosive used in formulation 4, and the simulation results are very different from the experimental results, which indicates that the parameters calculated by VLWR cannot be used for the aluminized explosives. Therefore, these parameters are needed to be adjusted for agreement with the experimental results, and the revised parameters of the RDX in aluminized explosives are obtained. Figure 5 shows that the numerical results obtained by using revised parameters are in good agreement with the experimental results. Table 2 lists the JWL equation of state parameters for RDX component of the aluminized explosives.

3.2 Experimental Fitting of Miller Reaction Rate Equation of Aluminum Particles

In the Miller reaction formulation, the value of *a* was obtained according to the reaction rate of the aluminum particles in the experiment. The aluminized explosives driving flyer experiment can be reproduced in LS-DYNA by using the JWL-Miller EOS. Through many attempts, when the value of *a* was set as 0.024, 0.032 and 0.055 corresponding to 50 μm, 5 μm and 50 nm aluminum particle size formulations respectively, so that the Miller reaction curve is closer to the actual reaction. As shown in Figure 6, the solid lines are the experimental results and the dashed lines are the numerical results calculated by Miller reaction, therefore, the fitting results are not ideal, and no matter what the value *a* is taken, the calculation results do not match with the experimental results. The differences are mainly in two aspects. The first one is that the variation trend of Miller reaction curves are quite different from the experimental curves. The Miller reaction curves are nearly linear, but the changes in the experimental reaction rate are not. For example, for 50 μm and 5 μm particles, the reaction rate increases firstly and then decreases. For 50 nm aluminum particles, its reaction rate reaches the maximum in the beginning, and then decreases, which indicates that the actual reaction mechanism of aluminum particles is quite complex. The reaction rate given by the Miller reaction formulation cannot reflect the actual reactions of aluminum in the detonation products. Another difference is that the deviation of the aluminum reaction degree is large, and the maximum deviation value is 20.8% and 41.9% for 50 μm and 5 μm aluminum particles. For 50 nm aluminum particles, the degree of reaction before 2.2 μs is the same, however the deviation increases from 2.2 μs.

It suggests that the Miller form of reaction rate equation is an empirical equation that does not consider the actual process of aluminum reactions, so it is not suitable for the analysis of aluminum particles reaction mechanism. In order to get more direct and objective reaction laws of aluminum particles, we consider a new reaction rate equation of aluminum particles to express the reaction rate of aluminum particles.

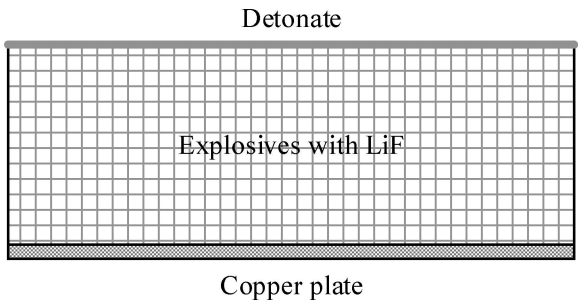

Figure 4. Copper flyer test model driven by LiF explosives.

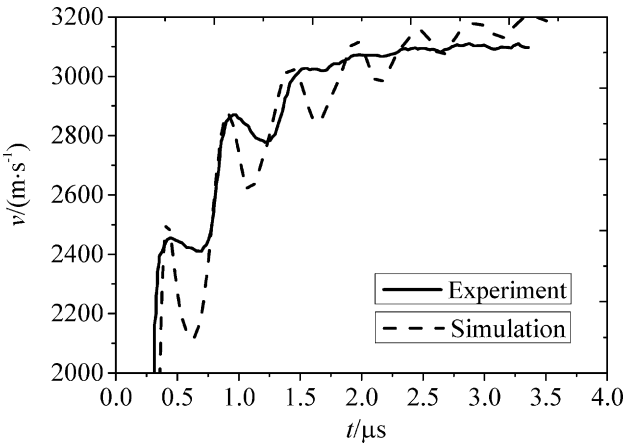

Figure 5. Simulated and test flyer velocity-time curves.

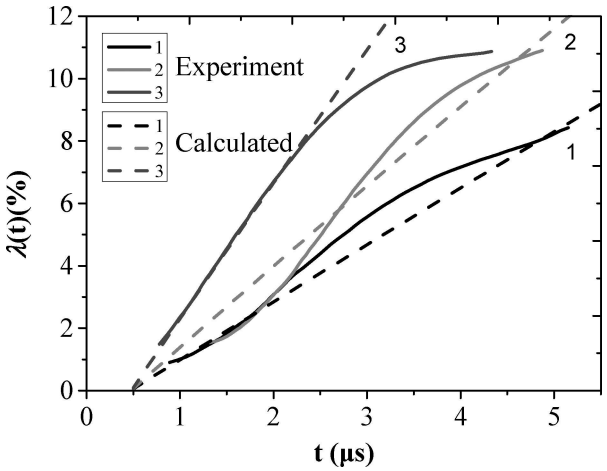

Figure 6. The Miller reaction form fitting with experimental results. 1. Ø50 μm aluminum particle 2. Ø5 μm aluminum particle 3. Ø50 nm aluminum particle.

3.3 The New Physical Model of Hypothesis, Derivation and Comparison with Experimental Data

The JWL EOS with the Miller extension has many advantages, however the empirical nature of the parameters in the extension requires an experimental calibration for every composition with different particle sizes of the aluminum component. The parameters cannot be calculated by the characteristics of aluminum particles. In order to obtain more intuitive and objective reactions of aluminum particles, we consider a new reaction rate equation for aluminum particles in combination with the JWL EOS.

It is assumed that the gasification of aluminum particles occurs in detonation products before all other reactions, and the released heat energy mainly depends upon the rate of the gasification reaction occurring during a relatively short period of time after CJ plane. According to the literature [14], the gasification time is between several microseconds to several tens of microseconds. However, we do not consider the diffusion of aluminum vapors, and the reactions between aluminum vapors and oxidizing gas occurs long after the CJ time. Therefore, the gasification rate of aluminum particles is used to replace the reaction rate in the detonation products.

According to the theory of molecular dynamics [18], the gasification rate equation of condense material can be written approximately as:

$$\dot{m}_v = \frac{\sqrt{3}}{2\pi r^3}\sqrt{kTm}e^{-E_v/RT} \tag{4}$$

where v is the average velocity of the molecule; $\dot{m}_v$ is kg/($m^2 \cdot s$); r is the radius of the molecule; k is t he Boltzmann constant, the value is 1.38×10^{-23} J/K; T is the temperature, the unit is K; m is the mass of each molecule; E_v is the gasification enthalpy; R is the gas constant, its value is 8.314 J/(mol·K).

The gasification process of spherical particles is given as:

$$\frac{d}{dt}\left[\frac{4}{3}\pi\left(\frac{d}{2}\right)^3\rho\right] = 4\pi\left(\frac{d}{2}\right)^2\dot{m}_v \tag{5}$$

$$d = d_0 - \frac{2\dot{m}_v}{\rho}t \tag{6}$$

where d is the particle diameter; d_0 is the initial particle diameter. It is further assumed that the aluminum particles in aluminized explosives exists mainly in the form of spherical particles, and the degree of reaction for aluminum particles can be written as:

$$\lambda = 1-(1-\frac{2\dot{m}_v t}{\rho_{Al}d_0})^3 = 1-\left(1-\frac{\sqrt{3KTm}}{\pi\rho_{Al}d_0 r^3}e^{-E_v/RT}t\right)^3 \tag{7}$$

We have assumed that the secondary reaction of the aluminum particles in the initial stage of the detonation is mainly the gasification of the aluminum particles. Therefore, the gasification reaction rate equation is used instead of the secondary reaction rate equation. By substituting Eq. (7) into Eq. (2), the final EOS of the aluminized explosives is obtained in the following form:

$$p = A\left(1-\frac{\omega}{R_1 v}\right)e^{-R_1 v} + B\left(1-\frac{\omega}{R_2 v}\right)e^{-R_2 v} + \frac{\omega\left(E+\left(1-\left(1-\frac{\sqrt{3KTm}}{\pi\rho_{Al}d_0 r^3}e^{-E_v/RT}t\right)^3\right)Q\right)}{v}. \tag{8}$$

For aluminized explosives, m is the mass of each molecule, r is the radius of the molecule, E_v is the gasification energy per mole; the parameters needed to be determined are A, B, R_1, R_2, ω and d_0.

For the three different particle sizes of aluminum constituents, the reactive degree of aluminum is expressed by Eq. (7). The parameters of this formulation are given above, where T is the temperature of the detonation products, which is a time dependent function. So Eq. (7) can be used to draw as a curve for each aluminum particle size formulation. The comparison between the calculated and experimental degree of reaction for the three aluminized formulations is shown in Figure 7.

It can be seen from Figure 7 that the experimental and calculated results are in good agreement. For each formulation the reaction rate of aluminum particles at the beginning of the reaction is maximum. This is because the reaction rate is proportional to the surface area of the particles, which is maximum at the start of reactions. Later on, the surface area of the particles continues to decrease until the aluminum particles react completely. The above

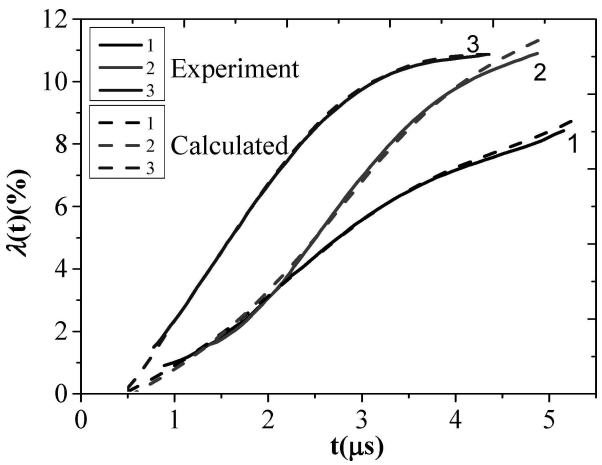

Figure 7. Comparing curves of numerical calculated and experimental reaction degrees of aluminum particles. 1. Ø50 μm aluminum particle 2. Ø5 μm aluminum particle 3. Ø50 nm aluminum particle.

Table 3. Computational parameters of Steinberg constitutive equation.

G_0/GPa	$b/(s^2\cdot kg^{2/3})$	$b'/(s^2\cdot kg^{2/3})$	H	f	$A(g\cdot mol^{-1})$	T_{m0}/K	γ_0	σ'_0/GPa
47.7	2.83	2.83	3.77×10^{-4}	0.001	63.55	1356	2.02	0.12

results show that the reaction rate equation of aluminum particles can reflect the reaction mechanism of aluminum particles in detonation products.

For the formulations with aluminum particle sizes of 5 μm and 50 μm, the reaction rate of the aluminum particles is initially slow, because at the initial stage the explosives have not detonated completely and the temperature of the detonation products is low. As the reactions progress, the product temperature rises and the reaction rate of the aluminum particles becomes faster and the aluminum particles participate in reactions at large scale. As the reactions continue, the detonation products expand, their temperature falls and the reaction rate begins to decrease. For the formulation with aluminum particle size of 50 nm, the reaction rate quickly reaches a constant value, and then the reaction rate decreases after 2.25 μs.

3.4 Numerical Simulation of Explosion-Driven Flyer by Different Size Aluminum Particles

The numerical simulation of the flyer driven by aluminized explosives was carried out by LS-DYNA. In order to compare the advantages of the new EOS to the JWL-Miller EOS, the two EOS with the aluminum reaction term were implemented to LS-DYNA, the simulation setup was the same as that of the test of LiF explosive driving flyer.

In the calculation, the copper flyer material was modeled by the Steinberg material model [19] given

$$G = G_0\left[1 + bpv^{1/3} - h\left(\frac{e-e_c}{3R'} - 300\right)\right]\exp\left(-\frac{f_e}{e_m - e}\right), \quad (9)$$

where G_0, b, h, f are the material constants determined for the experiment; p is the pressure; v is the specific volume; e_c is the cold compression energy; e_m is the melting energy; e is the specific internal energy; $R' = R\rho/A$, where R is the gas constant, ρ is density, A is molar mass. The yield strength is

$$\sigma_y = \sigma'_0\left[1 + b'pv^{1/3} - h\left(\frac{e-e_c}{3R'} - 300\right)\right]\exp\left(-\frac{fe}{e_m - e}\right), \quad (10)$$

where σ'_0 and b' are the material constants. The parameters of the constitutive model of Steinberg are shown in Table 3.

The Grüneisen equation of state was chosen for the copper flyer, given as

$$p = \frac{\rho_0 C^2\mu\left[1 + \left(1 - \frac{v_0}{2}\right)\mu - \frac{a}{2}\mu^2\right]}{\left[1 - (S_1 - 1)\mu + S_2\frac{\mu^2}{1+\mu} - S_3\frac{\mu^3}{(1+\mu)^2}\right]^2} + (\gamma_0 + a\mu)E, \quad (11)$$

where $\mu = \rho/\rho_0 - 1$; $v_0 = 1/\rho_0$; C is the intercept of Rankine-Hugoniot linear u_s–u_p; S_1, S_2, S_3 is the slope of line u_s–u_p; γ_0 is Grüneisen coefficient; a is the first order volume correction factor for γ_0. These parameters are seen in Table 4; and

Table 4. Parameters of Grüneisen equation of state of copper.

$\rho/(g\cdot cm^{-3})$	$C/(cm\cdot\mu s^{-1})$	S_1	S_2	S_3	γ_0	A
8.93	0.394	1.49	0	0	2.02	0.47

the parameters of the JWL-Miller and proposed EOS for aluminized explosives with different particle sizes are shown in Table 5.

The experiment of the flyer acceleration by aluminized explosives was calculated in LS-DYNA by using the JWL-Miller form of EOS and the simulation results are shown in Figure 8. In case of formulation 3 (the aluminized explosive with 50 μm aluminum particles), the calculated flyer velocity lags behind the experimental results after 2.5 μs. This is in accordance with the observation in Figure 6, where the reaction rate of aluminum particles calculated by using the JWL-Miller form of EOS lags behind the experimental values after 2.5 μs. The decrease in the energy released from aluminum reactions results in reducing the ability of flyer acceleration. The formulation 2 is similar to the case of formulation 3 (the aluminized explosive with 5 μm aluminum particles), the only difference in the transition time which is 2.75 μs in this case instead of 2.5 μs. However, for formulation 1 (the aluminized explosive with 50 nm aluminum particles), the calculated flyer velocity begins to increase from the experimental result after 2.2 μs. This is also in accordance with the observation in Figure 6, where the reaction rate of aluminum particles calculated by using the JWL-Miller form of EOS starts increasing from the experimental value after 2.2 μs. The increase in the energy released from aluminum reaction results in increasing the ability of flyer acceleration.

The experiment of the flyer acceleration by aluminized explosives was also calculated in LS-DYNA by using the newly proposed EOS and the simulation results are shown in Figure 9. The newly proposed EOS given in Eq. (6) describes the secondary reactions of aluminum particles, and the reaction rate of aluminum in aluminized explosives with

Table 5. Parameters of the JWL-Miller and proposed EOS for aluminized explosives with different particle sizes.

A/GPa	*B*/GPa	R_1	R_2	ω	d_0/μm	*Q*/(kJ/g)[20]	*a*	*m*/g	*r*/Å	E_v/(kJ/mol)
852	21	4.31	1.3	0.33	50	20.126	0.024	4.34e–26	1.82	300
852	21	4.31	1.3	0.33	5	20.126	0.032	4.34e–26	1.82	300
852	21	4.31	1.3	0.33	0.05	20.126	0.055	4.34e–26	1.82	300

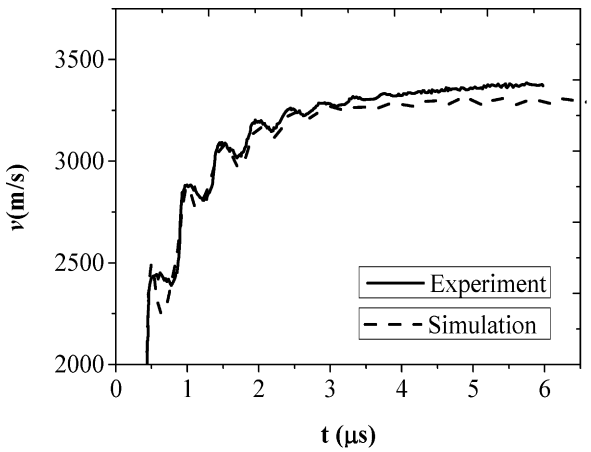

(a) 50 μm-sized aluminum particles

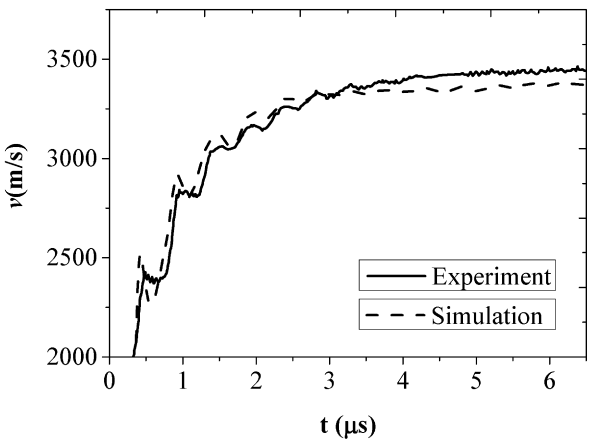

(b) 5 μm-sized aluminum particles

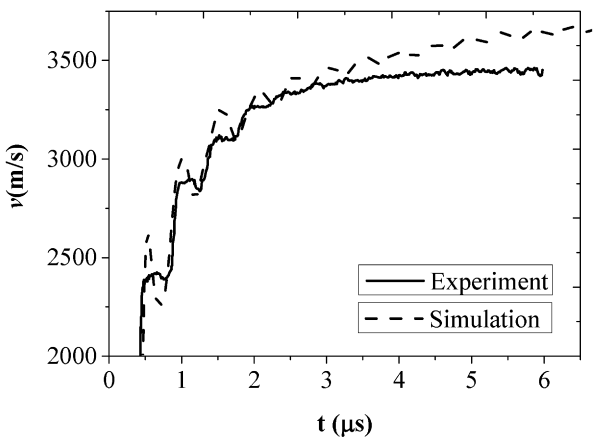

(c) 50 nm-sized aluminum particles

Figure 8. Simulated with JWL-Miller EOS and test velocity curves of copper flyer.

different aluminum particle sizes is confirmed by experiments. As it can be seen from Figure 9, for the copper flyer acceleration phenomenon, the calculated free surface velocity and experimental values are consistent, indicating that the newly proposed EOS appropriately describes the properties of the aluminized explosives.

During the detonation of aluminized explosives, aluminum particles react with the detonation products to release energy. In order to describe the effect of aluminum particle reactions on the work ability of aluminized explosives, the gasification rate equation of aluminum particles was added to the JWL equation of state. The new reaction rate model describes that the aluminum particles size has a significant effect on the detonation performance of the explosives.

From the numerical results, it can be concluded that in the reaction rate equation, the reaction rate of the aluminum particles increases with the decreases in their sizes. This is because the smaller aluminum particles more easily react with the detonation products, and thus the aluminum particles participate in the reactions at the early stages. Therefore, the amount of aluminum participating in the reactions at the early reaction stage increases, resulting in quick release of energy and consequently increasing the total energy release. For the aluminized explosives with alu-

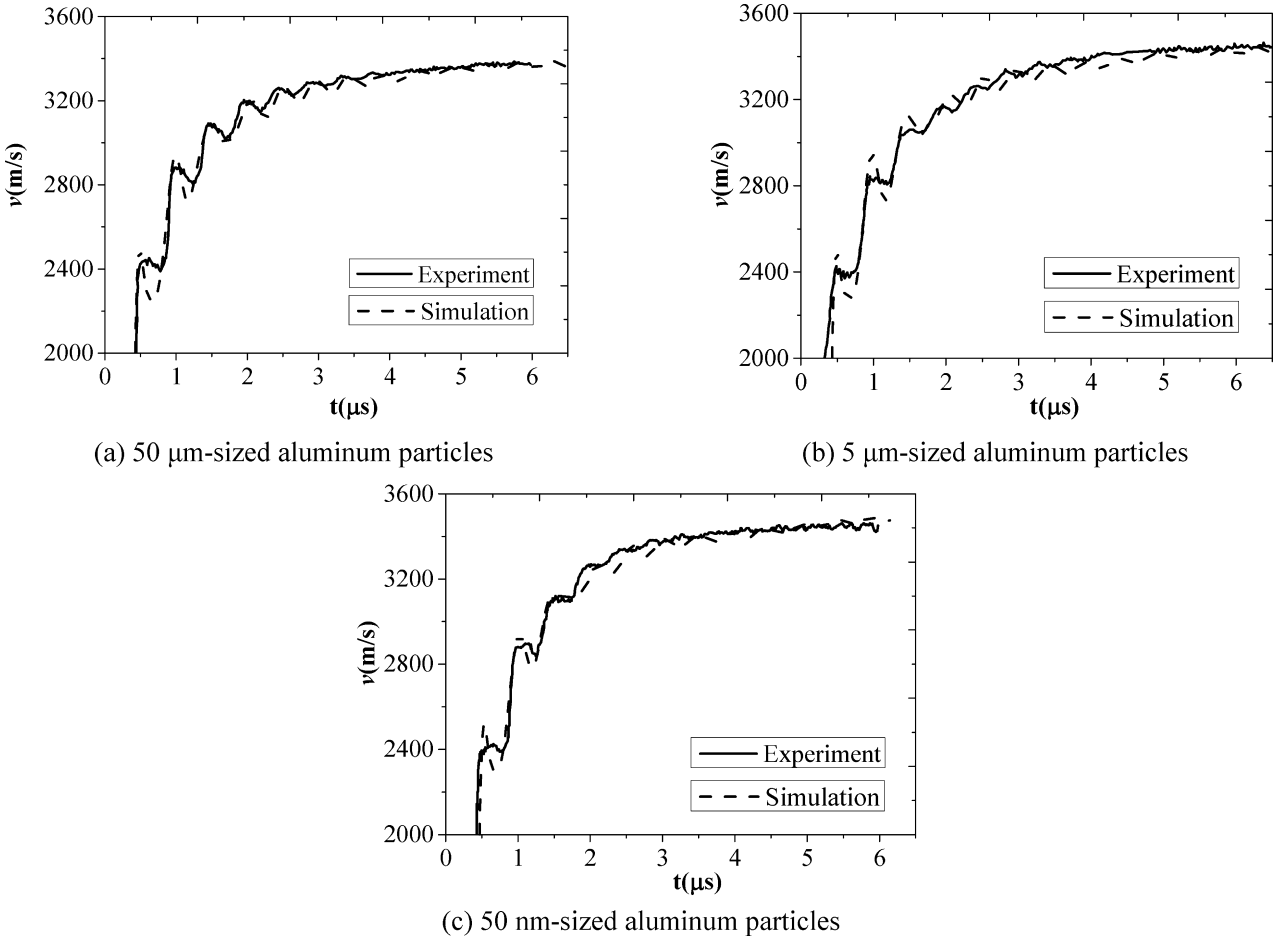

Figure 9. Simulated with the new EOS and test velocity curves of copper flyer.

minum particle sizes of micron scale, the reaction rate of aluminum particles first increases and then decreases. However, by addition of nano-sized aluminum particles into the explosive, the reaction rate quickly reaches a maximum value, because the reaction of nano-sized aluminum is easier. The good agreement of the calculated flyer velocity with that observed in experiments indicates that the newly proposed equation of state can better describe the detonation of aluminized explosives and reveals the mechanism of aluminum particle reactions. It better explains the work ability of the aluminized explosives with different sizes of aluminum particles. The equation of state proposed in the current paper may be of great significance to study the explosion of the aluminized explosives.

4 Conclusions

(1) The new EOS with the aluminum particle reaction term can reveal the detonation mechanisms of aluminized explosives. As the reactions between the aluminum particles and detonation products affects the released energy during detonation products expansion, the new EOS also explains why the aluminized explosive cylinder test is size dependent.

(2) Although the reactions between aluminum particles and detonation products are complicated, the calculated gasification rate of aluminum particles in this paper is consistent with the experimental results, which shows that it is reasonable assumption that the aluminum particles gasification of the RDX-based aluminized explosives can replace the actual aluminum particles reactions.

(3) The numerical results of the explosion-driving flyer velocity are consistent with the velocity curve of the flyer in the experiment, which shows that the new EOS suitably explains the energy release mechanism of the aluminized explosives and the validity of the rate equation of aluminum particles gasification is proved. With the decreases of the aluminum particle size, the energy release becomes faster, the total energy release of aluminized explosives increases and the expansion effect of explosives is enhanced.

(4) In aluminized explosives, as the aluminum particle size becomes smaller, the reaction rate increases. When the particle size of aluminum particles is at micron scale, the re-

action rate increases first and then decreases. For the nano-sized aluminum particles, the reaction rate quickly reaches to a constant value and then decreases. This indicates that the small size aluminum particles can react instantly and contribute to the total energy release in the detonation.

Acknowledgements

This paper is supported by National Natural Science Foundation of China (Grant No. 11872120 and 11521062).

References

[1] B. P. Zhang, Q. M. Zhang, F. L. Huang, *Detonation physics.* Beijing: Publishing House of Ordnance Industry, **2001**, p. 104–105.
[2] S. R. Yun, H. Y. Zhao, *Explosion mechanics.* Beijing: National Defense Industry Press, **2005**, P. 35–36.
[3] E. L. Lee, H. C. Hornig, J. W. Kury, *Adiabatic expansion of high explosive detonation products*, UCRL-50422. Livermore, CA, US: Lawrence Radiation Laboratory, **1968**.
[4] J. W. Kury, H. C. Honig, E. L. Lee, J. L. Mcdonnel, D. L. Ornellas, M. Finger, F. M. Strange, M. L. Wilkins, Metal acceleration by chemical explosives, *Proceedings of the 4th International Symposium on Detonation.* Washington DC, US: Office of Naval Research, Department of the Navy, **1965**, 3–13.
[5] M. Finger, H. C. Horning, E. L. Lee, J. W. Kury, Metal acceleration by composite HEs, *Proceedings of the 4th International Symposium on Detonation. Pasadena*, CA, US: Office of Naval Research, **1970**, 55–63.
[6] L. Chen, Y. M. Huang, C. G. Feng, The cylinder test and JWL equation of state detonation product of aluminized explosives, *Chin. J. Explos. Propellants* **2001**, *24*, 13–15.
[7] D. K. Ji, X. Z. Gao, C. Xiao, Study on dimension effect of accelerating ability and JWL equation of state for aluminized explosive, *Acta Armamentarii* **2012**, *33*, 552–555.
[8] X. L. Guo, Y. Han, S. J. Liu, L. C. Xiao, Experimental study on work ability of TATB-based aluminized explosives, *Chin. J. Explos. Propellants* **2015**, *38,* 81–85.
[9] E. L. Baker, V. Capellos, L. I. Stiel, J. Pincay, Accuracy and calibration of High Explosive Thermodynamic Equations of State, *J. Energ. Mater.* **2010**, *28*, 140–153.
[10] P. J. Miller, *A reactive flow model with coupled reaction kinetics for detonation and combustion in non-ideal explosives*, MRS (Materials Research Society), **1996**, p. 413–420.
[11] G. Yang, J. M. Zheng, D. A. Hu, Application of FE-SPH method to explosion in concrete by aluminized explosives, *Journal of Vibration and Shock* **2016**, *35*, 28–33.
[12] Z. Q. Zhou, J. X. Nie, X. Y. Guo, Q. S. Wang, Z. C. Ou, Q. J. Jie, A new method for determining the equation of state of aluminized explosive *Chin. Phys. Lett.* **2015**, *32*, 113–117.
[13] R. C. Ripley, L. Donahue, F. Zhang, Fragmentation of metal particles during heterogeneous explosion, *Shock Waves* **2015**, *25*, 151–167.
[14] H. B. Pei, Research on the reaction mechanism and energy release rule of aluminum powders in aluminized explosive, *Beijing: Beijing Institute of Technology* **2015**.
[15] L. Chen, Study of the metal acceleration capacities of aluminized explosives with spherical aluminum particles of different diameter, *Explosion and Shock Waves* **1999**, *19,* 250–254.
[16] D. Y. Liu, L. Chen, C. Wang, J. Y. Wu, Aluminum Acceleration and Reaction Characteristics for Aluminized CL-20-Based Mixed Explosives, *Propellants, Explosives, Pyrotechnics* **2018**, *43*, 543–551.
[17] L. Chen, C. G. Feng, X. P. Long, X. H. Jiang, *Aluminized explosives.* Beijing: National Defense Industry Press, **2004**, p. 132.
[18] R. P. Feynman, R. B. Leighton, M. Sands, *The Feynman Lectures on Physics (Volume I).* Pearson Education, **1989**, p. 433–437.
[19] D. J. Steinberg, *Equation of state and strength properties of selected materials.* Livermore, CA, US: Lawrence Livermore National Laboratory, **1991**.
[20] G. Baudin, D. Bergues, A reaction model for aluminized PBX applied to underwater explosive calculations, *Tenth Symposium (International) on Detonation.* Maryland, US Naval Surface Weapons Center, **1993**, 646–655.

Manuscript received: April 25, 2019
Revised manuscript received: May 4, 2019
Version of record online: July 11, 2019

